example, this is the case for water. This is consistent with the negative slope dP/dT of the crystal–liquid transition line for water, that implies that $\Delta S/\Delta V < 0$ since, according to the Clausius–Clapeyron equation, $dP/dT = \Delta S/\Delta V$, where ΔS and ΔV are the entropy and volume differences between the two coexisting phases.

For our system, we expect the reverse: $(\partial V/\partial T)_P > 0$ so $(\partial S/\partial V)_T > 0$, consistent with the positive slope of the LDL–HDL transition line dP/dT (see Fig. 2b). We confirm that $(\partial S/\partial V)_T > 0$ by explicitly calculating S for our system by means of thermodynamic integration.

Our results show that the presence of two critical points and the occurrence of the density anomaly are not necessarily related, suggesting that we might seek experimental evidence of a liquid–liquid phase transition in systems with no density anomaly. In particular, a second critical point may also exist in liquid metals that can be described by soft-core potentials. Thus the class of experimental systems displaying a second critical point may be broader than previously hypothesized. □

Received 6 October; accepted 18 December 2000.

1. Katayam, Y. *et al.* A first-order liquid–liquid phase transition in phosphorus. *Nature* **403,** 170–173 (2000).
2. Debenedetti, P. G. *Metastable Liquids: Concepts and Principles* (Princeton Univ. Press, Princeton, 1998).
3. Wilding, M. C., McMillan, P. F. & Navrotsky, A. The thermodynamic nature of a phase transition in yttria-alumina liquids. *J. Cryst. Noncryst. Solids* (in the press).
4. Brazhkin, V. V., Popova, S. V. & Voloshin, R. N. High-pressure transformations in simple melts. *High Pressure Res.* **15,** 267–305 (1997).
5. Brazhkin, V. V., Gromnitskaya, E. L., Stalgorova, O. V. & Lyapin, A. G. Elastic softening of amorphous H_2O network prior to the *HDA–LDA* transition in amorphous state. *Rev. High Pressure Sci. Technol.* **7,** 1129–1131 (1998).
6. Mishima, O. Liquid–liquid critical point in heavy water. *Phys. Rev. Lett.* **85,** 334–336 (2000).
7. Bellissent-Funel, M.-C. Evidence of a possible liquid–liquid phase transition in super-cooled water by neutron diffraction. *Nuovo Cimento* **20D,** 2107–2122 (1998).
8. Soper, A. K. & Ricci, M. A. Structures of high-density and low-density water. *Phys. Rev. Lett.* **84,** 2881–2884 (2000).
9. Lacks, D. J. First-order amorphous-amorphous transformation in silica. *Phys. Rev. Lett.* **84,** 4629–4632 (2000).
10. van Thiel, M. & Ree, F. H. High-pressure liquid–liquid phase change in carbon. *Phys. Rev. B* **48,** 3591–3599 (1993).
11. Poole, P. H., Sciortino, F., Essmann, U. & Stanley, H. E. Phase behavior of metastable water. *Nature* **360,** 324–328 (1992).
12. Glosli, J. N. & Ree, F. H. Liquid–liquid phase transformation in carbon. *Phys. Rev. Lett.* **82,** 4659–4662 (1999).
13. Saika-Voivod, I., Sciortino, F. & Poole, P. H. Computer simulations of liquid silica: Equation of state and liquid–liquid phase transition. *Phys. Rev. E* **63,** 011202-1–011202-9 (2001).
14. Mon, K. K., Ashcroft, M. W. & Chester, G. V. Core polarization and the structure of simple metals. *Phys. Rev. B* **19,** 5103–5118 (1979).
15. Stell, G. & Hemmer, P. C. Phase transition due to softness of the potential core. *J. Chem. Phys.* **56,** 4274–4286 (1972).
16. Silbert, M. & Young, W. H. Liquid metals with structure factor shoulders. *Phys. Lett.* **58A,** 469–470 (1976).
17. Levesque, D. & Weis, J. J. Structure factor of a system with shouldered hard sphere potential. *Phys. Lett.* **60A,** 473–474 (1977).
18. Kincaid, J. M. & Stell, G. Structure factor of a one-dimensional shouldered hard-sphere fluid. *Phys. Lett.* **65A,** 131–134 (1978).
19. Cummings, P. T. & Stell, G. Mean spherical approximation for a model liquid metal potential. *Mol. Phys.* **43,** 1267–1291 (1981).
20. Velasco, E., Mederos, L., Navascués, G., Hemmer, P. C. & Stell, G. Complex phase behavior induced by repulsive interactions. *Phys. Rev. Lett.* **85,** 122–125 (2000).
21. Voronel, A., Paperno, I., Rabinovich, S. & Lapina, E. New critical point at the vicinity of freezing temperature of K_2Cs. *Phys. Rev. Lett.* **50,** 247–249 (1983).
22. Behrens, S. H., Christl, D. I., Emmerzael, R., Schurtenberger, P. & Borkovec, M. Charging and aggregation properties of carboxyl latex particles: Experiments versus DLVO theory. *Langmuir* **16,** 2566–2575 (2000).
23. Debenedetti, P. G., Raghavan, V. S. & Borick, S. S. Spinodal curve of some supercooled liquids. *J. Phys. Chem.* **95,** 4540–4551 (1991).
24. Sadr-Lahijany, M. R., Scala, A., Buldyrev, S. V. & Stanley, H. E. Liquid state anomalies for the Stell-Hemmer core-softened potential. *Phys. Rev. Lett.* **81,** 4895–4898 (1998).
25. Jagla, E. A. Core-softened potentials and the anomalous properties of water. *J. Chem. Phys.* **111,** 8980–8986 (1999).
26. Stillinger, F. H. & Head-Gordon, T. Perturbational view of inherent structures in water. *Phys. Rev. E* **47,** 2484–2490 (1993).
27. Caccamo, C. Integral equation theory description of phase equilibria in classical fluids. *Phys. Rep.* **274,** 1–105 (1996).
28. Berendsen, H. J. C., Postma, J. P. M., van Gunsteren, W. F., DiNola, A. & Haak, J. R. Molecular dynamics with coupling to an external bath. *J. Chem. Phys.* **81,** 3684–3690 (1984).
29. Rein ten Wolde, P. & Frenkel, D. Enhancement of protein crystal nucleation by critical density fluctuations. *Science* **277,** 1975–1978 (1997).
30. Hagen, M. H. J., Meijer, E. J., Mooij, G. C. A. M., Frenkel, D. & Lekkerkerker, H. N. W. Does C_{60} have a liquid phase? *Nature* **365,** 425–426 (1993).

Acknowledgements

We wish to thank L. A. N. Amaral, P. V. Giaquinta, E. La Nave, T. Lopez Ciudad, S. Mossa, G. Pellicane, A. Scala, F. W. Starr, J. Teixeira, and, in particular, F. Sciortino for helpful suggestions and discussions. We thank the NSF and the CNR (Italy) for partial support.

Correspondence and requests for materials should be addressed to G.F. (e-mail: franzese@argento.bu.edu).

Strong radiative heating due to the mixing state of black carbon in atmospheric aerosols

Mark Z. Jacobson

Department of Civil & Environmental Engineering, Stanford University, Stanford, California 94305-4020, USA

Aerosols affect the Earth's temperature and climate by altering the radiative properties of the atmosphere. A large positive component of this radiative forcing from aerosols is due to black carbon—soot—that is released from the burning of fossil fuel and biomass, and, to a lesser extent, natural fires, but the exact forcing is affected by how black carbon is mixed with other aerosol constituents. From studies of aerosol radiative forcing, it is known that black carbon can exist in one of several possible mixing states; distinct from other aerosol particles (externally mixed[1–7]) or incorporated within them (internally mixed[1,3,7]), or a black-carbon core could be surrounded by a well mixed shell[7]. But so far it has been assumed that aerosols exist predominantly as an external mixture. Here I simulate the evolution of the chemical composition of aerosols, finding that the mixing state and direct forcing of the black-carbon component approach those of an internal mixture, largely due to coagulation and growth of aerosol particles. This finding implies a higher positive forcing from black carbon than previously thought, suggesting that the warming effect from black carbon may nearly balance the net cooling effect of other anthropogenic aerosol constituents. The magnitude of the direct radiative forcing from black carbon itself exceeds that due to CH_4, suggesting that black carbon may be the second most important component of global warming after CO_2 in terms of direct forcing.

This work was motivated by studies[1–7] that found different black-carbon (BC) forcings when different BC mixing states were assumed. In one study[7] the mixing state was found to affect the BC global direct forcing by a factor of 2.9 (0.27 $W m^{-2}$ for an external mixture, +0.54 $W m^{-2}$ for BC as a coated core, and +0.78 $W m^{-2}$ for BC as well mixed internally). Because BC is a solid and cannot physically be well mixed in a particle, the third case was discarded as unrealistic, and it was suggested that the real forcing by BC probably fell between that from an external mixture and that from a coated core. Here I report simulations that were performed among multiple aerosol size distributions to estimate which of these two treatments, if either, better approximates BC forcing in the real atmosphere.

The global model that I used was GATOR-GCMM, which treated gas, aerosol, radiative, meteorological and transport processes (see Supplementary Information for details). Aerosol processes included emissions, homogeneous nucleation, condensation, dissolution, coagulation, chemical equilibrium, transport, sedimentation, dry deposition, and rainout among 18 aerosol size distributions, 17 size bins per distribution, one number concentration, and an average of seven mole concentrations per bin per distribution. The 18 distributions (Supplementary Information) consisted of four 'primary' size distributions (sea spray (A), soil (B), black carbon (E1) and organic

matter (F)) into which emissions occurred, one 'primary' distribution (sulphate (D)) into which homogeneous nucleation occurred, two additional BC distributions (E2 and E3) into which primary BC grew, 10 'binary' distributions (AB, AD, AE, AF, BD, BE, BF, DE, DF and EF) that resulted from heterocoagulation among A, B, D, E1, E2, E3 and F distributions, and a completely mixed distribution (MX) that resulted from all higher heterocoagulation interactions. Distributions A, B, D, E1 and F were initialized, and the aerosol population was relaxed with continuous emissions that were allocated to distributions A, B, E1 and F, homogeneous nucleation that was allocated to distribution D, and coagulation, growth, chemistry, transport and deposition among all distributions until a near global-scale steady state was obtained.

Figure 1 shows the variation with time of the globally averaged mass per cent of BC-containing particles that obtained a non-BC coating of various mass percentages when (simulation a; Fig. 1a) coagulation alone and when (simulation b; Fig. 1b) coagulation, condensation, dissolution and equilibrium water uptake were the only forms of internal mixing. In the simulation shown in Fig. 1a, coagulation caused about 35% by mass of initial and emitted externally mixed BC to obtain a coating $>$ 20% by mass within five days. In the simulation shown in Fig. 1b, growth processes and coagulation together caused 63% of BC by mass to obtain a coating $>$ 20% by mass within five days. The difference indicates that growth and coagulation caused BC internal mixing at similar rates.

Coagulation has been calculated to affect the number and volume concentrations of particles primarily less than 0.2-μm diameter in urban air[8]. In that study, only one size distribution was considered. When multiple distributions are treated, the net effect of coagulation on the total number and volume concentrations of particles, summed over all distributions, is the same as that over one distribution if the initial number and volume concentrations are the same in both cases. The difference is that, in the multiple-distribution case, coagulation moves components among distributions (heterocoagulation), having a notable effect on particle composition not evident when only one distribution is simulated. Figure 2 shows such an effect. It shows the time-varying globally averaged mass per cent of BC in different distributions from the Fig. 1b simulation. Initially, all BC was externally mixed in distribution E1. BC then self-coagulated and grew into BC distributions E2 and E3 and heterocoagulated with sulphate, organic matter, soil and/or sea spray to form binary and higher mixtures. The difference between 100% and E1+E2+E3 in Fig. 2 represents the mass fraction of BC (50%) that heterocoagulated. Since this fraction is large, heterocoagulation appears to be important in the global-scale internal mixing of BC.

The mixing results that I report here seem to be consistent with

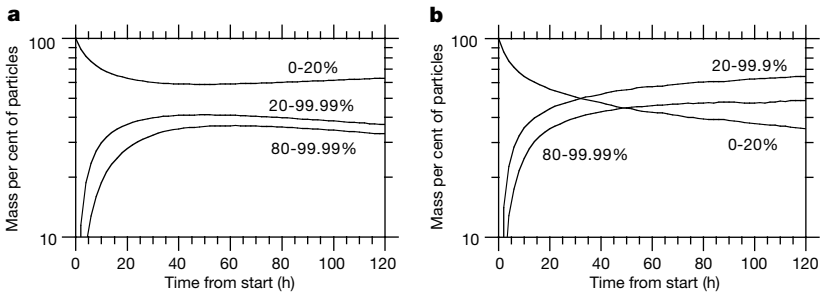

Figure 1 Coating of BC-containing particles over time. The figure shows the time-variation of the globally averaged mass per cent of BC-containing particles that obtain a non-BC coating of 0–20%, 20–99% and 80–99% by mass when (**a**) coagulation alone and (**b**) coagulation, condensation, dissolution, and equilibrium water uptake affect internal mixing. In both cases, emissions, homogeneous nucleation, transport, dry deposition, sedimentation, and rainout of aerosols were also treated. Initially, 100% by mass of BC-containing particles were externally mixed (containing 0% coating by mass). The percentages in the figure were obtained by summing, over all BC-containing distributions, the mass of BC-containing particles of a given shell mass fraction and normalizing by the total mass of BC-containing particles.

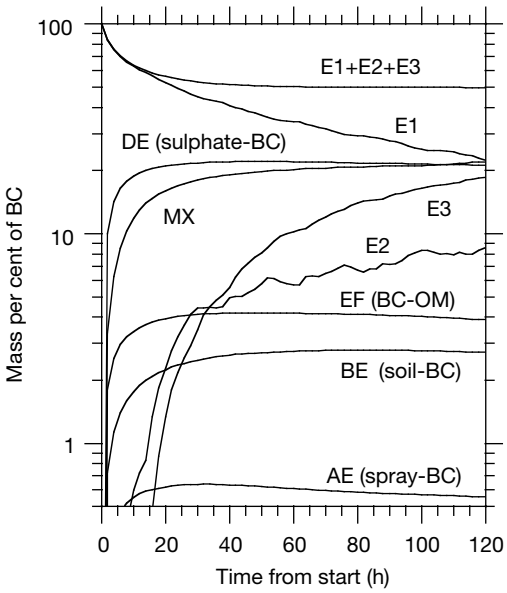

Figure 2 Shift of BC among particle distributions over time. The figure shows the globally averaged change in mixing state of BC among the 8 out of 18 size distributions in which BC was present, when coagulation, condensation, dissolution, and equilibrium water uptake affected internal mixing. Emissions, transport, dry deposition, sedimentation, and rainout of aerosols were also accounted for. Initially, all BC was externally mixed in distribution E1. Coagulation moved BC from distribution E1 to binary mixtures of sulphate-BC, BC-organic matter (OM), soil-BC and spray-BC, to ternary and higher mixtures (MX) and to distributions E2 and E3. Growth also contributed to moving material from E1 to E2 and E3.

observations. Andreae *et al.*[9] found that 80–90% of silicate particles over the Pacific Ocean between Ecuador and Hawaii contained sea spray. Here, by five days, 70–85% of soil particles in this region contained sea spray. Murphy *et al.*[10] found that almost all particles $>0.13\,\mu m$ over the remote Southern Pacific Ocean contained sea spray. Here, >95% of all near-surface particles in that region contained sea spray. Posfai *et al.*[11] found that almost all soot particles over the North Atlantic contained sulphate. Here, >93% of BC-containing particles in this region contained sulphate.

Simulations were run to estimate the yearly and globally averaged radiative effects of treating BC in three ways: as a coated core in multiple distributions; as a single externally mixed distribution; and as a coated core in a single internally mixed distribution (Fig. 3). In the multiple-distribution case, modelled mid-visible optical depths (0.1–0.4) and single-scattering albedos (0.86–0.97) over the eastern United States and the western Atlantic Ocean during TARFOX were in the range of measured values (0.06–0.7 and 0.85–0.98, respectively; refs 12, 13). Modelled optical depths (0.16–0.44) in the Arabian Sea, and optical depths (0.07–0.17) and single-scattering albedos (0.88–0.94) in the Indian Ocean during INDOEX were similarly close to observations (0.2–0.4 (ref. 14), ≤ 0.1 (ref. 14) and 0.88–0.90 (ref. 15), respectively). Modelled mid-visible single-scattering albedos over biomass-burning regions of Brazil (0.86–0.94) were in the range of measurements obtained during the same time of year (0.82–0.94 (ref. 16), 0.79–0.95 (ref. 17). Modelled single-scattering albedos over biomass-burning regions of Africa (0.85–0.92) were close to those over biomass-burning regions of Brazil. The modelled annually averaged mid-visible optical depth over the global oceans (0.13) compares with a measured value of 0.12 (ref. 18).

Figure 3 shows that, within five days, the BC forcing from the multiple-distribution coated-core case was within 24% of that from the single-distribution coated-core case. This implies that the single-distribution coated-core assumption appears to be a better approximation of BC direct forcing than is the external-mixture assumption. As all studies to date have used the external-mixture assumption for determining lower bounds or average values of global direct forcing by anthropogenic aerosols, such lower bounds or average values must be higher (closer to zero) than all previous studies have predicted.

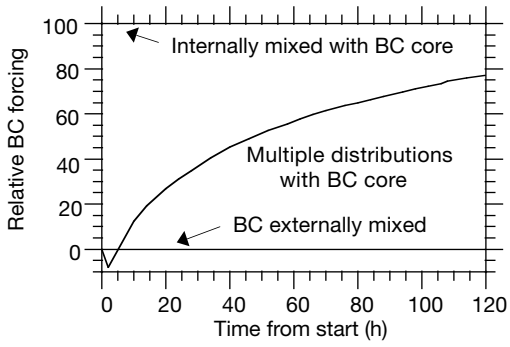

Figure 3 Time-dependent relative global BC direct forcing (at the tropopause) obtained when 18 size distributions were modelled. The relative forcing is $(F_{mult} - F_{ext}) / (F_{int} - F_{ext})$, where F_{mult}, F_{ext} and F_{int} are the forcings obtained with multiple distributions with BC as core, a single externally mixed BC distribution, and a single internally mixed distribution with BC as core, respectively. Each of the three forcing values at each time was calculated by averaging results from 24 simulations (6 days per year and 4 start times per day). For each simulation, the multiple-distribution forcing was obtained by initializing externally mixed distributions and relaxing towards a steady state with continuous emissions and nucleation of externally mixed particles and physical/chemical/deposition processes among all particles. The single externally and internally mixed distributions were derived from the multiple-distribution cases each time step in a mass-conserving manner to guarantee that the mass of BC and other components were exactly the same in each size bin each time step. Radiative calculations were then performed over the single distributions.

The final yearly averaged direct forcing due to BC in the external mixture, the multiple-distribution coated-core, and the single internally-mixed, coated-core distribution cases from Fig. 3 were 0.31, 0.55 and $0.62\,W\,m^{-2}$, respectively. The multiple-distribution BC direct forcing (0.55) falls between direct-forcing estimates for CH_4 ($0.47\,W\,m^{-2}$) and CO_2 ($1.56\,W\,m^{-2}$) from IPCC[19]. Thus, subject to uncertainties, BC may be the second most important component of global warming in terms of direct forcing, after CO_2. For this reason, controls on BC emissions, not treated under the Kyoto Protocol of December 1997, need to be considered. Major sources of BC include the burning of diesel fuel, coal, jet fuel, natural gas, and biomass.

Previous studies have implied[7] or suggested[20] that BC controls would be beneficial (studies have also shown that controls on non-CO_2 greenhouse-gas emissions would be beneficial[21]). The present study suggests that BC controls may be as—or more—beneficial than methane controls. Nevertheless, to obtain the true effect on rising global temperatures of controls on BC, CH_4 and CO_2, comparative time-dependent simulations of the response of climate to these pollutants are needed. □

Received 24 July; accepted 23 November 2000.

1. Haywood, J. M., Roberts, D. L., Slingo, A., Edwards, J. M. & Shine, K. P. General circulation model calculations of the direct radiative forcing by anthropogenic sulfate and fossil-fuel soot aerosol. *J. Clim.* **10,** 1562–1577 (1997).
2. Haywood, J. M. & Ramaswamy, V. Global sensitivity studies of the direct radiative forcing due to anthropogenic sulfate and black carbon aerosols. *J. Geophys. Res.* **103,** 6043–6058 (1998).
3. Myhre, G., Stordal, F., Restad, K. & Isaksen, I. S. A. Estimation of the direct radiative forcing due to sulfate and soot aerosols. *Tellus B* **50,** 463–477 (1998).
4. Cooke, W. F., Liousse, C., Cachier, H. & Feichter, J. Construction of a 1°×1° fossil fuel emission data set for carbonaceous aerosol and implementation and radiative impact in the ECHAM4 model. *J. Geophys. Res.* **104,** 22137–22162 (1999).
5. Hansen, J. E. *et al.* Climate forcings in the industrial era. *Proc. Natl Acad. Sci. USA* **95,** 12753–12758 (1998).
6. Penner, J. E., Chuang, C. C. & Grant, K. Climate forcing by carbonaceous and sulfate aerosols. *Clim. Dyn.* **14,** 839–851 (1998).
7. Jacobson, M. Z. A physically-based treatment of elemental carbon optics: Implications for global direct forcing of aerosols. *Geophys. Res. Lett.* **27,** 217–220 (2000).
8. Jacobson, M. Z. Development and application of a new air pollution modeling system - II. Aerosol module structure and design. *Atmos. Environ.* **31,** 131–144 (1997).
9. Andreae, M. O. *et al.* Internal mixture of sea salt, silicates, and excess sulfate in marine aerosols. *Science* **232,** 1620–1623 (1986).
10. Murphy, D. M. *et al.* Influence of sea-salt on aerosol radiative properties in the Southern Ocean marine boundary layer. *Nature* **395,** 62–65 (1998).
11. Posfai, M., Anderson, J. R., Buseck, P. R. & Sievering, H. Soot and sulfate aerosol particles in the remote marine troposphere. *J. Geophys. Res.* **104,** 21685–21693 (1999).
12. Hegg, D. A., Livingston, J., Hobbs, P. V., Novakov, T. & Russell, P. Chemical apportionment of aerosol column optical depth off the mid-Atlantic coast of the United States. *J. Geophys. Res.* **102,** 25293–25303 (1997).
13. Russell, P. B., Hobbs, P. V. & Stowe, L. L. Aerosol properties and radiative effects in the United States East Coast haze plume: An overview of the tropospheric aerosol radiative forcing observational experiment (TARFOX). *J. Geophys. Res.* **104,** 2213–2222 (1999).
14. Jayaraman, A. *et al.* Direct observations of aerosol radiative forcing over the tropical Indian Ocean during the January-February 1996 pre-INDOEX cruise. *J. Geophys. Res.* **103,** 13827–13836 (1998).
15. Satheesh, S. K. *et al.* A model for the natural and anthropogenic aerosols over the tropical Indian Ocean derived from Indian Ocean Experiment data. *J. Geophys. Res.* **104,** 27421–27440 (1999).
16. Eck, T. F., Holben, B. N., Slutsker, I. & Setzer, A. Measurements of irradiance attenuation and estimation of aerosol single scattering albedo for biomass burning aerosols in Amazonia. *J. Geophys. Res.* **103,** 31865–31878 (1998).
17. Dubovik, O. *et al.* Single-scattering albedo of smoke retrieved from the sky radiance and solar transmittance measured from ground. *J. Geophys. Res.* **103,** 31903–31923 (1998).
18. Husar, R. B., Prospero, J. M. & Stowe, L. L. Characterization of tropospheric aerosols over the oceans with the NOAA advanced very high resolution radiometer optical thickness operational product. *J. Geophys. Res.* **102,** 16889–16909 (1997).
19. Houghton, J. T. *et al.* (eds) *Climate Change 1995, The Science of Climate Change* (Cambridge University Press, New York, 1996).
20. Hansen, J., Sato, M., Ruedy, R., Lacis, A. & Oinas, V. Global warming in the twenty-first century: An alternative scenario. *Proc. Natl Acad. Sci.* **97,** 9875–9880 (2000).
21. Hayhoe, K. *et al.* Costs of multigreenhouse gas reduction targets for the USA. *Science* **286,** 905–906 (1999).

Supplementary information is available on *Nature*'s World-Wide Web site (http://www.nature.com) or as paper copy from the London editorial office of *Nature*.

Acknowledgements

This work was supported by the NASA New Investigator Program, the NSF, the David and Lucile Packard Foundation, and Hewlett-Packard.

Correspondence and requests for information should be addressed to author (e-mail: jacobson@ce.stanford.edu).